Inorganic Chemistry

Article

pubs.acs.org/IC

$A_6U_3Sb_2P_8S_{32}$ (A = Rb, Cs): Quinary Uranium(IV) Thiophosphates Containing the $[Sb(PS_4)_3]^{6-}$ Anion

Jean-Marie Babo,[‡] Kariem Diefenbach,[†] and Thomas E. Albrecht-Schmitt*,[†]

[†]Department of Chemistry and Biochemistry, Florida State University, 95 Chieftan Way, Tallahassee, Florida 32306-4390, United States

[‡]Department of Civil & Environmental Engineering and Earth Sciences, University of Notre Dame, Notre Dame, Indiana 46556, United States

Supporting Information

ABSTRACT: The reaction of $A_2S_3/U/P_2S_5/S$ at 500 °C affords the quinary U(IV) thiophosphates $A_6U_3Sb_2P_8S_{32}$ (A = Rb, Cs). These compounds contain $\{U_3(PS_4)_2[Sb(PS_4)_3]_2\}^{6-}$ layers separated by alkali metal cations. The layers are composed of trimeric uranium units connected to each other by the thiophosphato-antimonite anion, $[Sb(PS_4)_3]^{6-}$. This unit contains a central Sb(III) cation bound by three $[PS_4]^{3-}$ anions, creating a trigonal pyramidal environment around Sb(III). Each uranium cation is surrounded by eight sulfides in a distorted square antiprism that shares two edges with two other US_8 units to form a trimeric $[U_3S_{18}]^{24-}$ cluster. Magnetic susceptibility measurements indicate that the close proximity of the U(IV) within these clusters leads to antiferromagnetic ordering at 53 K. Reflectance spectroscopy indicates that these compounds are semiconductors with a band gap of 1.48 eV.

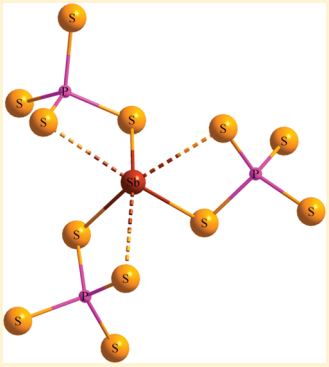

INTRODUCTION

The chemistry of thiophosphate and its heavier congeners is typically more complex than $[PO_4]^{3-}$ because the heavier chalcogenides often catenate to form polychalcogenide units, and chalcophosphates often condense into polymeric substructures, whereas phosphate is usually monomeric.[1−5] Linear, ramified, cyclic, and infinite chain-building units containing P_2Q_6, P_2Q_9, P_2Q_{10}, P_4Q_{13}, P_6Q_{12}, and PQ_6 are known.[3,4,6−8] The condensation of tetrahedral PQ_4 units yields moieties with structures and stereochemistries reminiscent of both simple and complex hydrocarbons. These complex anions form glasses[1,9−11] and molecular, 1D, 2D, and 3D architectures, although 3D frameworks are the most common.[1,3,4,6] In addition, because the synthetic conditions employed in the preparation of these compounds is highly reducing, the possibility of oxidation states lower than +5 for phosphorus, and the formation of P−P bonds, is known to occur.[3,4,8]

The chalcophosphates are capable of binding a vast array of main group, transition metal, and f block cations in both low and high oxidation states.[12−16] Among the richest group of these compounds are those that contain uranium. Their complexity can be ascribed to several factors. First, the uranium brings structural intricacy to these systems in that the coordination chemistry of uranium is extremely flexible and coordination numbers of eight and nine are typical. Second, the oxidation state of uranium can vary between +4 and +6. Third, the uranium cations stabilize a wide variety of thiophosphate anions, leading to immense structural complexity and new main group chemistry. Examples of this include $Rb_4U_4P_4Se_{26}$, which contains uranium in the atypical +5 oxidation state, and $A_{11}U_7(PS_4)_{13}$ (A = K, Rb), which despite containing only isolated $[PS_4]^{3-}$ anions forms a fascinating architecture constructed from interlocked helices.[13,17]

The possibility of creating even more complex thiophosphate anions exists by incorporating additional chalcophilic main group elements. One such element is antimony,[16] which under these synthetic conditions will be Sb(III) and will therefore possess a lone-pair of electrons that is likely to be stereochemically active, leading to rich structural chemistry. Herein we present the synthesis, structure elucidation, and properties of the quinary U(IV)/Sb(III) thiophosphates $A_6U_3Sb_2P_8S_{32}$ (A = Rb, Cs), which contain the new $[Sb(PS_4)_3]^{6-}$ anion.

EXPERIMENTAL SECTION

Synthesis. $A_6U_3Sb_2P_8S_{32}$ (A = Rb, Cs) were synthesized by reacting a mixture of $A_2S_3/U/P_2S_5/S$ in 1:1:2:1 stoichiometric ratio in an evacuated silica glass tube with an outer diameter of 10 mm (the total mass of mixture was 917 mg). This sealed ampule was then slowly heated to 500 °C over 24 h, held there for 5 days, and then slowly cooled to room temperature at the rate of 5 °C/h. Dark red irregular-shaped crystals of the title compounds formed together with unavoidable yellowish $A_3Sb(PS_4)_2$ (A = Rb, Cs)[18] byproducts with almost the same density and yield (50% based on Sb metal). The crystals were obtained by isolation in degassed dimethylformamide (DMF) and dry ethanol. For further analyses, the crystals of these compounds were hand-picked. Attempts to increase the yield by modification of stoichiometry or reaction conditions were unsuccessful. Moreover, the use of AN_3 as alkali metal source as previously

Received: December 11, 2013
Published: March 14, 2014

   dx.doi.org/10.1021/ic403044x | Inorg. Chem. 2014, 53, 3540−3545

reported[19] significantly decreased the formation of crystals of both the desired compounds and the byproducts.

Crystal Structure Determination. Single-crystal X-ray diffraction data were collected at room temperature on a Bruker APEXII CCD X-ray diffractometer using graphite-monochromatized Mo Kα radiation. The data were corrected for Lorentz and polarization effects.[20] Multiscan absorption corrections were done using the SADABS program. The structures of both compounds were solved by direct methods and refined in full-matrix least-squares with the aid of the SHELXTL package of crystallographic programs.[21] Selected crystallographic details can be found in Table 1. Selected bond distances and angles are provided in Tables 2 and 3.

Table 1. Selected Crystallographic Data for $A_6U_3Sb_2P_8S_{32}$ (A = Rb, Cs)

	$Rb_6U_3Sb_2P_8S_{32}$	$Cs_6U_3Sb_2P_8S_{32}$
cryst syst	trigonal	trigonal
space group	$R\bar{3}c$	$R\bar{3}c$
unit cell params a/Å	14.906(1)	44.895(3)
c/Å	14.985(1)	46.139(4)
formula unit per unit cell (Z)	6	6
calcd density[a] (D_x in g/cm^3)	3.17	3.36
molar volume[a] (V_m in cm^3/mol)	867.03	900.19
index range ($\pm h_{max}/\pm k_{max}/\pm l_{max}$)	19/19/58	19/19/59
$2\theta_{max}$ (in deg)	54.92	49.62
$F(000)$	7392.0	8040.0
absorp coeff (μ in mm^{-1})	15.77	13.93
collected reflns	8404	8310
unique reflns	2215	1732
R_{int}/R_σ	0.064/0.045	0.107/0.062
reflns with $\lvert F_o\rvert \geq 4\sigma(F_o)$	1877	1388
R_1/R_1 with $\lvert F_o\rvert \geq 4\sigma(F_o)$[a]	0.026/0.023	0.032/0.028
wR_2 (for all reflections)[b]	0.083	0.095
goodness of fit (GooF)	1.082	1.344
residual electron density max./min. ρ (e$^-$ × 10^6 pm^{-3})	3.370/−1.800	2.135/−1.629

[a] $R(F) = \sum\lvert\lvert F_o\rvert - \lvert F_c\rvert\rvert/\sum\lvert F_o\rvert$. [b] $R(F_o^2) = [\sum w(F_o^2 - F_c^2)^2/\sum w(F_o^4)]^{1/2}$.

Table 2. Selected Bond Distances (Å) and Angles (deg) in $Rb_6U_3Sb_2P_8S_{32}$

U−S1 (×2)	2.924(1)	P1−S1 (×3)	2.066(2)
U− S1′ (× 2)	2.934(1)	S6	1.967(3)
U− S3 (× 2)	2.738(1)	P2 − S2	2.074(2)
U− S5 (× 2)	2.791(2)	−S3	2.051(3)
		−S4	1.993 (2)
Rb− S1	4.033(1)	−S5	2.037(2)
Rb−S2	3.592(1)	Sb − S2 (× 3)	2.542(2)
Rb− S2′	3.639(1)	−S4 (× 3)	3.012(2)
Rb−S3	3.518(1)	S2−Sb−S2	89.43(6)
Rb−S3′	3.873(1)	S4−Sb−S4	112.88(6)
Rb−S4	3.457(1)	S1−P1−S1	104.27(8)
Rb−S4′	3.474(1)	S1−P1−S6	114.27(7)
Rb−S5	3.766(1)	S2−P2−S4	112.74(9)
Rb−S6	3.570(1)	S3−P2−S4	108.08(9)
		S4−P2−S5	113.13(9)

Solid-State UV−Vis−NIR Spectroscopy. The absorption spectra of the title compounds were collected from single crystals at room temperature using a Craic Technologies UV−vis−NIR microspectrometer in the 200−1500 nm region.

Elemental Analysis. Semiquantitative elemental analyses were measured using a field emission scanning electron microprobe (LEO EVO 50) equipped with an Oxford INCA energy dispersive X-ray spectrometer (EDX). EDX data were collected from several crystals of the same compound, and the presence of all the elements A, U, Sb, S, and P was detected in the samples.

Table 3. Selected bond distances (Å) and angles (deg) in $Cs_6U_3Sb_2P_8S_{32}$

U−S1 (×2)	2.936(2)	P1−S2	2.054(2)
U−S1′ (×2)	2.950(2)	P1−S3	2.076(2)
U−S2 (×2)	2.746(2)	P1−S4	1.997(2)
U−S5 (×2)	2.790(1)	P1−S5	2.038(3)
		P2−S1 (×3)	2.067(2)
Cs1−S1	4.235(2)	P2−S6	1.971(4)
Cs1−S2	3.737(2)	Sb−S1 (×3)	2.552(2)
Cs1−S2′	3.757(2)	Sb−S4 (×3)	3.007(2)
Cs1−S3	3.617(2)	S1−Sb−S1	88.76(9)
Cs1−S3′	3.951(2)	S4−Sb−S4	112.67(6)
Cs1−S4	3.541(2)	S2−P1−S3	108.20(13)
Cs1−S4′	3.571(2)	S2−P1−S4	107.94(13)
Cs1−S5	3.738(2)	S3−P1−S4	106.294(102)
Cs2−S6	3.622(2)	S1−P2−S1	104.62(10)
Cs1−S1 (×2)	3.489(2)	S1−P2−S6	113.97(8)
Cs1−S2 (×2)	3.232(2)		
Cs1−S5 (×2)	3.721(2)		

Raman Spectroscopy. Raman spectra were collected on single crystals of $A_6U_3Sb_2P_8S_{32}$ (A = Rb, Cs) using a Bruker Sentinel system linked via fiber optics to a video-assisted Raman probe in a microscope mount. The laser wavelength was 750 nm with a power of 400 mW, while the collection was made between 100 and 700 cm^{-1}. The instrument is equipped with a high-sensitivity, TE-cooled 1024 × 255 CCD array.

Magnetic Property Measurements. The direct current (dc) magnetic susceptibility was measured as a function of temperature using a Quantum Design MPMS SQUID magnetometer. A 4.3 mg sample of polycrystalline $Cs_6U_3Sb_2P_8S_{32}$ was placed in a gelatin capsule, secured by diamagnetic tape within a commercial straw, for which all diamagnetic contributions were accounted for. For a typical temperature sweep experiment, the sample was cooled to 1.8 K under zero-field cooled (ZFC) conditions. The data were collected by heating the sample from 1.8 to 300 K under various applied fields. The data were also collected by field cooling (FC). Finally, measurements at 1.8 K were conducted by measuring the magnetic susceptibility as a function of field, up to 70 000 Oe.

RESULTS AND DISCUSSION

Structure Elucidation. $A_6U_3Sb_2P_8S_{32}$ (A = Rb, Cs) possess similar structures and are nearly isotypic. Both contain $[U_3(PS_4)_2[Sb(PS_4)_3]_2]^{6-}$ layers intercalated by A^+ cations. The only structural difference is that the interlayer cations are disordered with cesium, with two crystallographic positions, whereas the rubidium compound is fully ordered, and the Rb center resides on a single crystallographic site. The layers are rotated as they stack along the c-axis by 30° as a consequence of $\bar{3}$ symmetry, and this leads to a very long axis. The layers are composed of trimeric uranium units connected to each other by the $[Sb(PS_4)_3]^{6-}$ anion. Each uranium cation is surrounded by eight sulfide anions in a distorted square antiprism that shares two edges with two other crystallographically equivalent units to form a trimeric $[U_3S_{18}]^{24-}$ cluster as shown in Figure 1. The trigonal prismatic cavities created at the center of the clusters are capped by two $[PS_4]^{3-}$ anions. This trimer is different from other edge-sharing uranium(IV) polyhedra reported by Reynolds et al.[22] The U_3S_{18} building units further share common edges with the $[Sb(PS_4)_3]^{6-}$ anions to form the

dx.doi.org/10.1021/ic403044x | Inorg. Chem. 2014, 53, 3540−3545

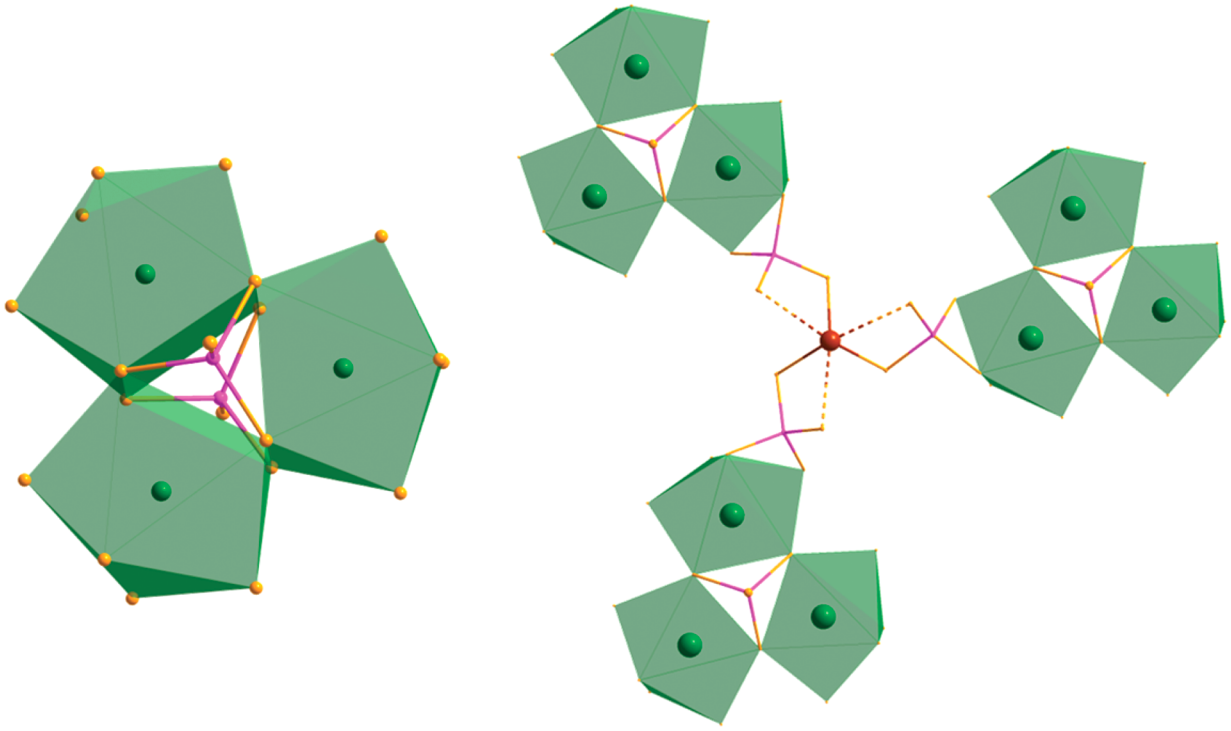

Figure 1. The $[U_3S_{18}]^{24-}$ trimer capped by two $[PS_4]^{3-}$ units (left) and their further connection by the $[Sb(PS_4)_3]^{6-}$ anion (right).

anionic layers, $[U_3(PS_4)_2[Sb(PS_4)_3]_2]^{6-}$, with the A^+ cations residing between them (see Figure 2).

The new $[Sb(PS_4)_3]^{6-}$ anion is created by binding a central Sb(III) cation with three $[PS_4]^{3-}$ anions, creating a trigonal pyramidal environment around Sb(III). This environment indicates that the lone-pair on Sb(III) is stereochemically active. However, as is often the case with these types of lone-pair systems, additional longer interactions take place between the Sb(III) centers and the three $[PS_4]^{3-}$ anions, and therefore the antimony environment is better described as a 3 + 3 distorted octahedral environment.

The U−S distances range from 2.738(2) to 2.949(2) Å (see Tables 2 and 3) and are in good agreement with those of 2.734(2)−2.989(2) Å found in ternary thiophosphates, UP_2S_7 and UP_2S_9, or 2.725(4) to 2.980(4) Å observed in $Cs_8U_5(P_3S_{10})_2(PS_4)_6$.[6] The trimer units found in the title compounds have also been reported in some quaternary thiophosphates, such as $Cs_8U_5(P_3S_{10})_2(PS_4)_6$, where they are further connected to $[US_8]^{12-}$ polyhedra via $[PS_4]^{3-}$ and $[P_3S_{10}]^{5-}$ anions, and then into frameworks or the interlocking inorganic helices of $A_{11}U_7(PS_4)_{13}$[17] via $[PS_4]^{3-}$ and $[US_9]$. This is the first time that this trimeric unit is isolated in its simplest representation. The geometry and the size of the thiophosphate ligand may have favored this isolation.

The Sb−S bonds in the $[Sb(PS_4)_3]^{6-}$ anion range between 2.542(1) and 2.547(2) Å, while the three longer secondary contacts are from 3.008(2) to 3.012(2) Å. Comparatively, in the isolated trigonal pyramidal SbS_3 unit, the Sb−S distances are shorter: 2.366(1) to 2.438(1) Å in $[Cr(1.3\text{-dap})_2SbS_3]$,[23] for example. The $[PS_4]^{3-}$ units in the $[Sb(PS_4)_3]^{6-}$ anions are slightly distorted with P−S distances ranging from 1.997(3) to 2.076(3) Å and S−P−S angles from 107.697(10) to 112.927(11)°, but remain in good agreement with many other values reported. However, the isolated $[(P2)S_4]^{3-}$ group exhibits an equilateral face that caps the trimeric cluster void. Its terminal S4 atom tilts away, causing a deformation of the tetrahedron. In contrast, the doubly chelating $[(P1)S_4]^{3-}$ anion is distorted by the Sb(III) lone-pair of electrons.

The two crystallographic unique cesium positions are surrounded by nine and six sulfides with distances that range from 3.541(2) to 4.236(2) Å and 3.230(2) to 3.720(2) Å, respectively. The unique rubidium site is surrounded by nine sulfides with Rb−S distances ranging between 3.474(1) and 4.033(1) Å. Although the two cesium positions are not fully occupied, the occupancy factor of the six-coordinated site is very low. The low coordination number of this cesium site is a consequence of the steric effects of the $[Sb(PS_4)_3]^{6-}$ anions (see Figure 3c) and leads to somewhat large thermal motion of these cations, as revealed by a high thermal displacement parameter value of 0.0661(31) $Å^2$.

UV−Vis−NIR Spectroscopy. Reflectance data generated for each compound were used to estimate the band gaps by converting reflectance spectra to absorption with the Kubelka−Munk function. These data were then compared with known compounds to aid in the assignment of the oxidation state of uranium in these compounds. The analyses of both spectra suggest 1.48 eV band gaps for both compounds (see Figure S1). These compounds are consequently semiconductors. However, there are some difficulties in separating the band edges from the f−f transitions. The two spectra show relatively intense peaks near 1 eV, and these transitions are consistent with the assigned f−f transitions for U(IV). Similar transitions are observed for the U(IV) chalcogenides, $Cs_8U_5(P_3S_{10})_2(PS_4)_6$ and RbU_2SbSe_8.[6,13] Comparison of these spectra with other U(IV) thiophosphates confirms the +4 oxidation state of uranium[1,2] and reinforces the results of the bond-valence calculations (see Table S1). The large irregular shape of crystals of $A_6U_3Sb_2P_8S_{32}$ (A = Rb, Cs) results in their much darker color compared to the lath-shaped crystals of UP_2S_9.[1]

dx.doi.org/10.1021/ic403044x | Inorg. Chem. 2014, 53, 3540−3545

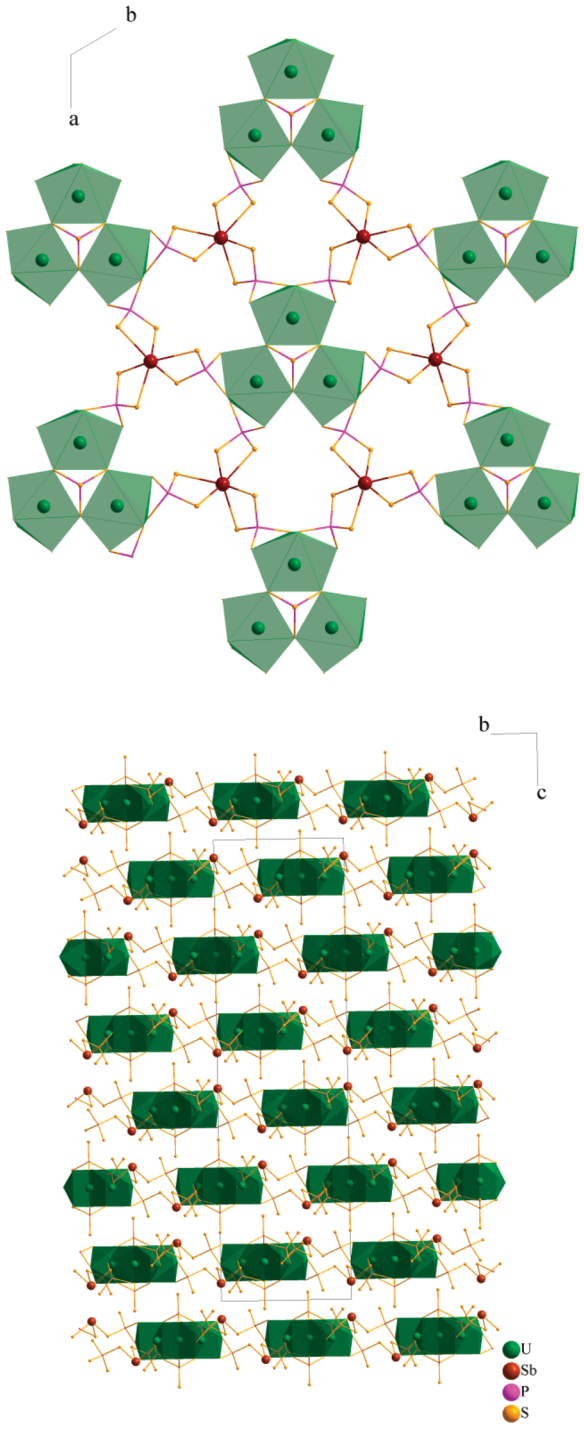

Figure 2. Part of a $[U_3(PS_4)_2[Sb(PS_4)_3]_2]^{6-}$ layer (top) stacking perpendicularly to the *c*-axis in the $A_6U_3Sb_2P_8S_{32}$ (A = Rb, Cs) crystal structure (bottom).

Raman Spectroscopy. The Raman spectra of both compounds reveal very similar patterns (see Figure S2). Reported values of $[PS_4]$, as well as larger $[P_2S_7]$ or $[P_3S_{10}]$ units, yield vibrational stretches in the ranges of 200−300 and 400−650 cm^{-1}. There is some overlap with Sb−S stretching modes which are active from 150 to 400 cm^{-1}.[1,13,24] The presence of both P−S and Sb−S entities in these compounds leads to possible overlap of peaks in the 150−650 cm^{-1} region. However, the Sb−S modes could be identified exclusively within the 300−400 cm^{-1} region, where the P−S vibrations seem not to be specifically active. In the $Rb_6U_3Sb_2P_8S_{32}$ spectrum, two peaks were found near 310 and 330 cm^{-1} and were assigned to Sb−S stretching modes. The characteristic peaks concomitantly found in both spectra near 190, 260, and 410 cm^{-1} can be assigned to P−S modes. The latter peaks were also found for UP_2S_9, UP_2S_7, $K_{1.5}Bi_{2.5}(PS_4)_3$, and $ASnPS_4$ (A = K−Cs).[1,10,25]

Magnetism Behavior. Uranium(IV) exhibits a $5f^2$ configuration, and based on Russell−Saunders coupling, it is classified as a non-Kramer ion with a $^3H_4$ ground state. Strong magnetic anisotropy is well known to occur in uranium(IV)-containing compounds.[26,27] The temperature dependence of the molar magnetic susceptibility, χ_M, was measured after zero field cooling to 1.8 K and measuring the susceptibility up to 300 K as shown in Figure 4. A sharp cusp was noted at approximately 53 K, which may occur due to magnetic ordering or perhaps spin frustration occurring within the uranium trimers. However, this feature is close that found when O_2 leaks into magnetometers, which prompted measurements under a variety of conditions, repeated measurements on the same and different compounds and different sample containers, and even measurements on different SQUIDS.[28,29] Field-cooled and ZFC measurements at field strengths of 1000, 2000, and 10000 Oe were then carefully conducted on the sample on different days to reduce the chance of oxygen being in the system and producing the aforementioned peak. The results from all measurements maintain the distinct peak observed at 53 K, boosting our confidence in claiming the peak to arise from the trimers of uranium (see Figures S3 to S5 for further plots).

The effective moment is defined as $\mu_{eff} = g(J(J + 1))^{1/2}$, where J is the Russell−Saunders full angular momentum yielding U(IV) a $J = 4$ magnetic spin ground level and a theoretical free-ion moment of 3.58 μ_B. Magnetic susceptibility can be represented by $\chi = (C/T - \theta)$, the Curie−Weiss law, where C is the Curie constant related to the effective moment by $\mu_{eff} = (3kC/N\mu_B^2)^{1/2}$, and θ is the Weiss constant, which is interpreted as a temperature offset to adjust for lower temperature moment correlations. N indicates Avogadro's number, and k represents the Boltzmann constant. The data do not obey Curie−Weiss behavior at low temperatures near the observed transition because they are based on a mean-field approximation, but fitting to our $1/\chi_M$ vs T plot in the linear range 75 to 150 K (see Figure 4) yields an effective moment of 6.1(9) μ_B and a Weiss constant of $\theta = -113$ K, which is in good accordance with the expected free ion moment of 6.20 μ_B for three U(IV) ions, assuming Russell−Saunders coupling of a $^3H_4$ ground level. A magnetization plot is provided in Figure 5.

Field sweep measurements up to 70 000 Oe were conducted on the polycrystalline $Cs_6U_3Sb_2P_8S_{20}$ at 1.8 K (see Figure 5), nearly saturating at 1 μ_B per formula unit, indicating the magnetic ions are antiferromagnetically coupled. The negative Weiss constant, $\theta = -113$ K, supports the spins being antiferromagnetically aligned.

CONCLUSIONS

Ordered quinary compounds are rare because it is difficult to find five different elements that are chemically compatible, yet also have distinct coordination chemistry. $A_6U_3Sb_2P_8S_{32}$ (A = Rb, Cs) are ordered because each element possesses both complementary bonding aspects and divergent geometric requirements. U(IV), Sb(III), and P(V) all form strong bonds with sulfur and are known to be chalcophilic. Yet each of these elements possesses a very different chemical environ-

dx.doi.org/10.1021/ic403044x | Inorg. Chem. 2014, 53, 3540−3545

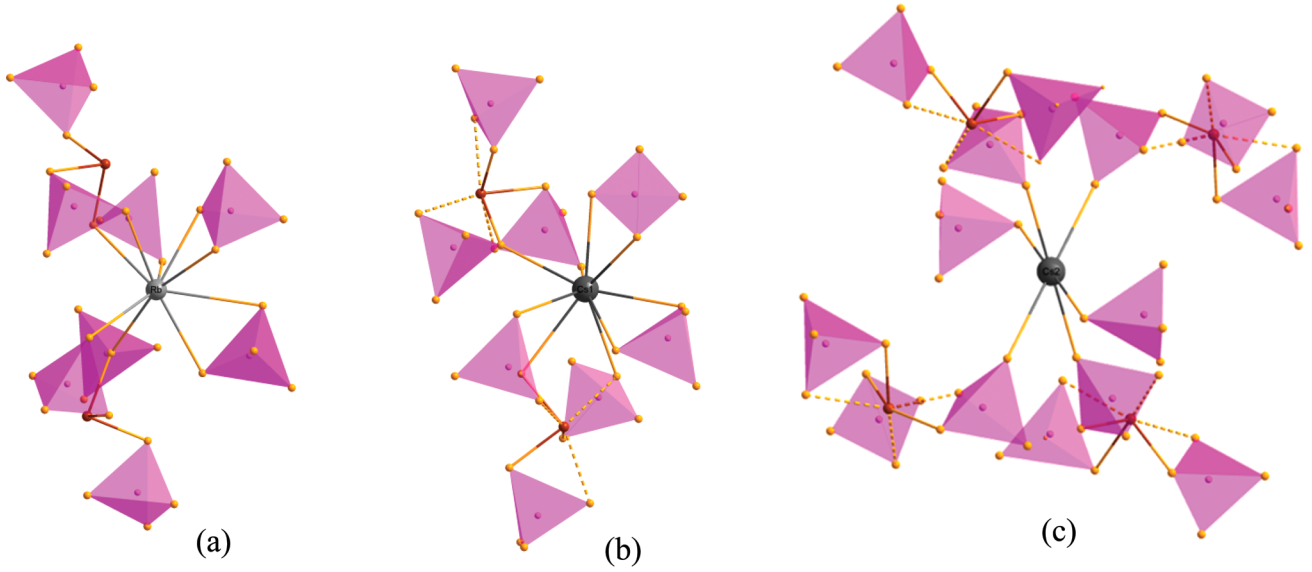

Figure 3. Alkali-metal coordination environment in $A_6U_3Sb_2P_8S_{32}$ (A = Rb, Cs) for (a) Rb^+, (b) $(Cs1)^+$, and (c) $(Cs2)^+$.

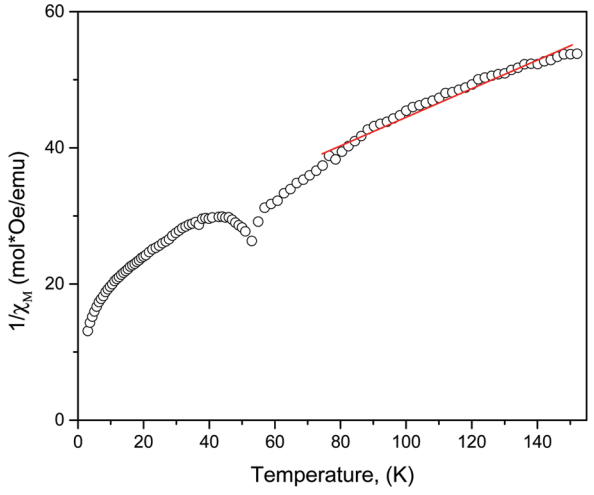

Figure 4. Temperature dependence of the inverse magnetic susceptibility, $1/\chi_M$, of $Cs_6U_3Sb_2P_8S_{20}$. The zero field cooled measurement was done under a field of 0.1 T. The red line shows the fit in the range of 75 to 150 K to the Curie–Weiss law. The fitting results in an effective moment of 6.1(9) μ_B and a Weiss constant of θ = −113.

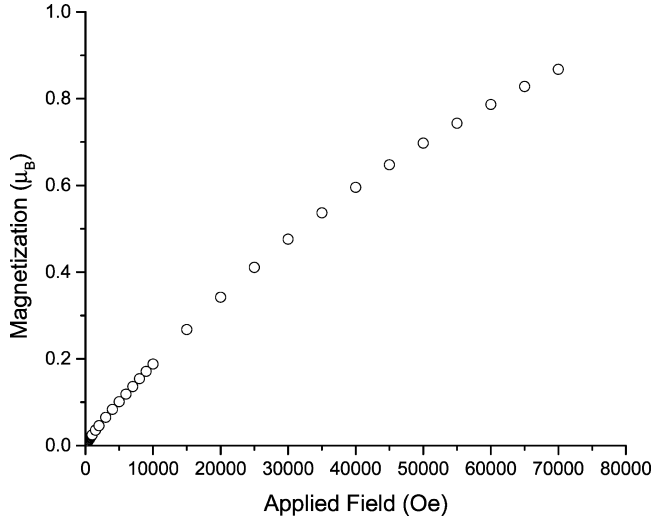

Figure 5. Magnetization of $Cs_6U_3Sb_2P_8S_{20}$ obtained at 1.8 K with a field from 0 Oe up to 70 000 Oe.

ment. U(IV) is present in an eight-coordinate square antiprism, Sb(III) is a trigonal pyramid, and P(V) in a tetrahedron, all combined via bridging sulfide anions. Alternatively, one might look at the structure from the point of view of the coordination flexibility of thiophosphate as a distinct building unit. Here instead we can think of the $[PS_4]^{3-}$ anion as an excellent ligand for both U(IV) and Sb(III). As is typically found, an anionic structure forms and the alkali metal cations, whose bonding is purely ionic and is therefore distinct from the other four elements, balances charge and fills void space. It is interesting that the $[Sb(PS_4)_3]^{6-}$ anion creates a rather open structure that in turns forces the U(IV) centers to cluster. The U(IV) centers in the trimers are antiferromagnetically coupled, revealing a well-defined peak at 53 K.

■ ASSOCIATED CONTENT

Ⓢ Supporting Information

X-ray crystallographic files in CIF format. This material is available free of charge via the Internet at http://pubs.acs.org.

■ AUTHOR INFORMATION

Corresponding Author

*E-mail: talbrechtschmitt@gmail.com.

Notes

The authors declare no competing financial interest.

■ ACKNOWLEDGMENTS

This work was supported by the National Science Foundation through DMR-1004459. A portion of this work was performed at the National High Magnetic Field Laboratory, which is supported by the National Science Foundation Cooperative Agreement No. DMR-0084173, by the State of Florida, and by the Department of Energy.

REFERENCES

(1) Babo, J.-M.; Jouffret, L. J.; Jian, L.; Villa, E. M.; Albrecht-Schmitt, T. E. *Inorg. Chem.* **2013**, *52*, 7747−7751.
(2) Hess, R. F.; Gordon, P. L.; Tait, C. D.; Abney, K. D.; Dorhout, P. K. *J. Am. Chem. Soc.* **2002**, *124*, 1327−1333.
(3) Wu, Y.; Bensch, W. *Inorg. Chem.* **2007**, *46*, 6170−6177.
(4) Cody, J. A.; Finch, K. B.; Reynders, G. J., III; Alexander, G. C. B.; Lim, H. G.; Naether, C.; Bensch, W. *Inorg. Chem.* **2012**, *51*, 13357−13362.
(5) Fragnaud, P.; Evain, M.; Prouzet, E.; Brec, R. *J. Solid State Chem.* **1993**, *102*, 390−399.
(6) Hess, R. F.; Abney, K. D.; Burris, J. L.; Hochheimer, H. D.; Dorhout, P. K. *Inorg. Chem.* **2001**, *40*, 2851−2859.
(7) Gieck, C.; Rocker, F.; Ksenofontov, V.; Tremel, W. *Angew. Chem., Int. Ed.* **2011**, *40*, 908−911.
(8) Chondroudis, K.; Kanatzidis, M. G. *Inorg. Chem.* **1998**, *37*, 2098−2099.
(9) Larink, D.; Eckert, H.; Martin, S. W. *J. Phys. Chem. C* **2012**, *116*, 22698−22710.
(10) Banerjee, S.; Malliakas, C. D.; Kanatzidis, M. G. *Inorg. Chem.* **2012**, *51*, 11562−11573.
(11) Berbano, S. S.; Seo, I.; Bischoff, C. M.; Schuler, K. E.; Martin, S. W. *J. Non-Cryst. Solids* **2012**, *358*, 93−98.
(12) Wu, Y.; Naether, C.; Bensch, W. *Inorg. Chem.* **2006**, *45*, 8835−8837.
(13) Choi, K.-S.; Kanatzidis, M. G. *Chem. Mater.* **1999**, *11*, 2613−2618.
(14) Babo, J.-M.; Albrecht-Schmitt, T. E. *J. Solid State Chem.* **2012**, *187*, 264−268.
(15) Malonis, J. M.; Kanatzidis, M. G. *J. Am. Chem. Soc.* **2012**, *134*, 16441−16446.
(16) Zhao, H.-J.; Li, L.-H.; Wu, L.-M.; Chen, L. *Inorg. Chem.* **2010**, *49*, 5811−5817.
(17) Gieck, C.; Tremel, W. *Chem.—Eur. J.* **2002**, *8*, 2980−2987.
(18) McCarthy, T.; Kanatzidis, M. G. *J. Alloys Compd.* **1996**, *236*, 70−85.
(19) Babo, J.-M.; Choi, E. S.; Albrecht-Schmitt, T. E. *Inorg. Chem.* **2012**, *51*, 11730−11735.
(20) *SAINT*, version 4; Siemens Analytical X-ray Systems, Inc.: Madison, WI, 1996.
(21) Sheldrick, G. M. *SHELXTL*, version 5; Siemens Analytical X-ray Systems, Inc.: Madison, WI.
(22) Reynolds, J. G.; Zalkin, A.; Templeton, H. D.; Edelstein, N. M. *Inorg. Chem.* **1977**, *16*, 599−603.
(23) Seidlhofer, B.; Spetzler, V.; Naether, C.; Bensch, W. *J. Solid State Chem.* **2012**, *187*, 269−275.
(24) Piccoli, B. P. M.; Abney, K. D.; Schoonover, J. D.; Dorhout, P. K. *Inorg. Chem.* **2001**, *40*, 4871−4875.
(25) Gave, M. A.; Weliky, D. P.; Kanatzidis, M. G. *Inorg. Chem.* **2007**, *46*, 11063−11074.
(26) De Boer, F. R. *Phys. B: Condens. Matter* **1989**, *155*, 221−224.
(27) Arko, A. J.; Joyce, J. J.; Havela, L. In *The Chemistry of Actinide and Transactinide Elements*, 3rd ed.; Morss, R., Edelstein, N. M., Fuger, J., Eds.; Springer: Dordrecht, The Netherlands, 2006; Vol. *4*, pp 2307−2379.
(28) Jeżowski, A.; Litwicki, Z.; Sumarokov, V. V.; Stachowiak. *Low Temp. Phys.* **2006**, *32*, 1082−1085.
(29) Klotz, S.; Strässle, T.; Cornelius, A. L.; Philippe, J.; Hansen, T. *Phys. Rev. Lett.* **2010**, *104*, 115501(1)−115501(4).